

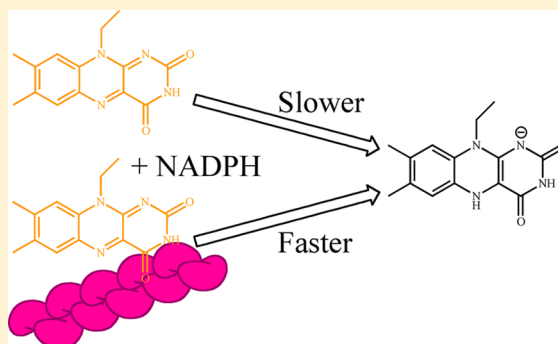
## Actin Stimulates Reduction of the MICAL-2 Monooxygenase Domain

Claudia A. McDonald,<sup>†</sup> Ying Yi Liu, and Bruce A. Palfrey\*

Department of Biological Chemistry, University of Michigan Medical School, 1150 West Medical Center Drive, Ann Arbor, Michigan 48109-0606, United States

**ABSTRACT:** MICALs are large, multidomain flavin-dependent monooxygenases that use redox chemistry to cause actin to depolymerize. Little enzymology has been reported for MICALs, and none has been reported for MICAL-2, an enzyme vital for the proliferation of prostate cancer. The monooxygenase domains of MICALs resemble aromatic hydroxylases, but their substrate is the sulfur of a methionine of actin. In order to determine how closely MICAL-2 conforms to the aromatic hydroxylase paradigm, we studied its reaction with NAD(P)H. The enzyme has a strong preference for NADPH over NADH caused by a large difference in binding NADPH. A comparison of the reduction kinetics using protio-NADPH and [4R-<sup>2</sup>H]-NADPH showed that MICAL-2 is specific for the *proR* hydride of NADPH, as evidenced by a 4.8-fold kinetic isotope effect.

The reductive half-reaction of the MICAL-2 hydroxylase domain is stimulated by f-actin. In the absence of actin, NADPH reduces the flavin relatively slowly; actin speeds that reaction significantly. The separate monooxygenase domain of MICAL-2 has the classic regulatory behavior of flavin-dependent aromatic hydroxylases (Class A monooxygenases): slow reduction of the flavin when the substrate to be oxygenated is absent. This prevents the wasteful consumption of reduced pyridine nucleotide and the production of harmful H<sub>2</sub>O<sub>2</sub>. Our results show that this strategy is used by MICAL-2. Thus, our data suggest that MICAL-2 could regulate catalysis through the monooxygenase domain alone; control by interactions with other domains of MICAL in the full-length enzyme may not be needed.



MICALs are large, multidomain flavin-dependent monooxygenases that use redox chemistry to cause actin to depolymerize.<sup>1,2</sup> The actin cytoskeleton is fundamentally important for most cellular developmental processes. MICAL is vital in the development of axons<sup>3</sup> and the viability of prostate cancer cells.<sup>4</sup> There are three MICAL isozymes found in vertebrates: MICAL-1, MICAL-2, and MICAL-3. All MICALs have an N-terminal flavin-dependent monooxygenase domain (monoMICAL) (Figure 1) followed by a calponin homology region (CH domain) and a LIM domain. MICAL-1 has two more domains after the LIM domain: a proline-rich region and coiled-coils. MICAL-3 is missing the proline-rich region but has four domains including the coiled coils. MICAL-2 only has three domains (Figure 1). Studies on *Drosophila* have demonstrated that the flavin of the monooxygenase domain of MICAL is vital for its signal transduction function.<sup>3</sup> Some enzymology has been reported for MICALs,<sup>5</sup> but none has been reported for MICAL-2. Detailed mechanistic enzymological studies are needed to understand how this monooxygenase causes actin depolymerization.

The key intermediate in flavin monooxygenase chemistry is the flavin hydroperoxide. The hydroperoxide is a versatile reagent, able to oxygenate nucleophiles or electrophiles.<sup>6</sup> The hydroperoxide is produced on the enzyme by the reaction of reduced flavin with dioxygen. Reduced flavin is produced by the reaction of oxidized flavin with reduced pyridine nucleotide. Monooxygenases regulate catalysis in different ways.<sup>6</sup> Regu-

lation is important because the flavin hydroperoxide is unstable and if no substrate is present, it will eventually decay to oxidized flavin and hydrogen peroxide, producing a toxin and wasting valuable reducing equivalents. Different classes of monooxygenases have different regulatory strategies. The aromatic hydroxylases (Class A)<sup>7</sup> do not allow rapid flavin reduction unless the substrate is present. In contrast, the Class B monooxygenases rapidly react with NAD(P)H and O<sub>2</sub> but stabilize the hydroperoxide.

monoMICAL has properties of both the aromatic hydroxylases and the Class B monooxygenases. The structure of the monooxygenase domain of MICAL is very similar to aromatic hydroxylases such as *p*-hydroxybenzoate hydroxylase (PHBH).<sup>8,9</sup> Aromatic hydroxylases like PHBH have a unique flavin conformational change; the flavin moves from a buried "in" conformation to an exposed "out" conformation.<sup>6</sup> These conformational changes were also observed in the crystal structures of monoMICAL-1.<sup>8,9</sup> In the structure of the oxidized monooxygenase domain, the flavin is in the "out" conformation (Figure 1). In the structure of the reduced monooxygenase domain, the flavin adopts both conformations. In contrast to its structural similarities to aromatic hydroxylases, monoMICAL-1 has been found to oxygenate Met44 on f-actin, making

Received: February 7, 2013

Revised: July 12, 2013

Published: August 8, 2013

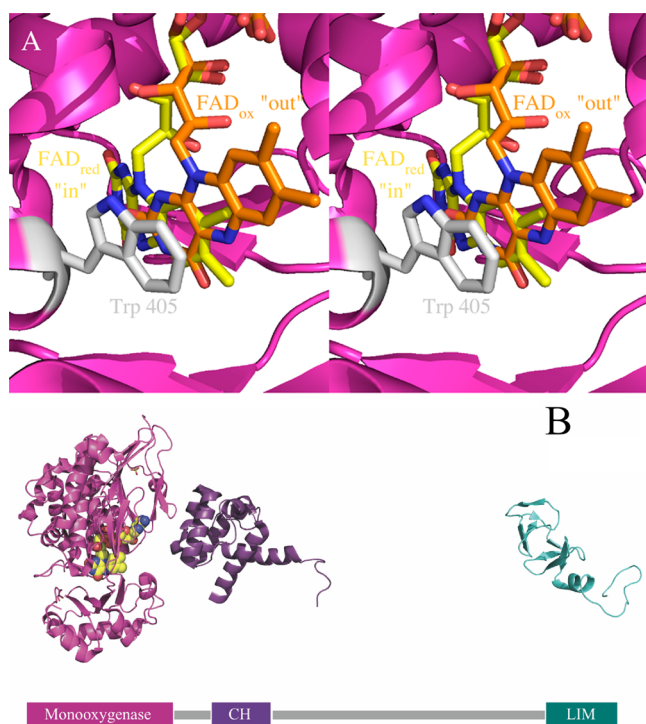


**Figure 1.** Structures of MICAL. (A) Active sites of oxidized and reduced human monoMICAL-1. The “in” conformation of the flavin, from the structure of the reduced enzyme (PDB 2C4C), is shown in yellow. The “out” conformation of the oxidized enzyme is shown in orange (PDB 2BRY). Note Trp 405 (platinum), which stacks on the isoalloxazine in the “out” conformation. (B) Domains of MICAL-2. The N-terminal monooxygenase domain of MICAL-2, shown in pink, is followed by the CH domain in purple and the C-terminal LIM domain in cyan. Cartoons of the structures of each domain (PDB 2BRY, 2DK9, and 1IML) are placed above their position in the domain diagram (not to scale) after the fashion of Siebold et al.<sup>8</sup>

methionine sulfoxide.<sup>10</sup> The oxygenation of thioethers by Class B monooxygenases is well known, but that reaction has never been reported for aromatic hydroxylases. Therefore, monoMICAL is uniquely exhibiting characteristics of both groups.

A detailed examination of the steps in the catalytic cycle is needed to further learn which group monoMICAL most resembles, an important first step in uncovering the regulation of the chemistry by cellular signals. The reductive half-reaction is a key difference between the two groups of monooxygenases. Here, we examine the reductive half-reaction kinetically to find out which model of regulation applies to monoMICAL. We find that monoMICAL-2 reacts with NADPH slowly, but in the presence of f-actin, reduction is stimulated. monoMICAL-2 has a preference for NADPH over NADH. Similar to aromatic hydroxylases, monoMICAL-2 transfers the *pro-R* hydride of NADPH.

## EXPERIMENTAL PROCEDURES

**Expression Construct.** To construct the pMICAL-2 plasmid, the segment of the MICAL-2 gene encoding the monooxygenase domain of MICAL-2 (residues 1–494) from *Mus musculus* was cloned from Mammalian Gene Collection MICAL-2 cDNA Clone ID 40061128 (Thermo Scientific). The monoMICAL-2 gene was amplified using primers 5′-TACTTC-CAATCCAATGCCATGGGAGAGAATGAAGATGAGAAG

and 5′-TTATCCAATTCCAATGCTAGTCCATCTCCT-TAGTGATGTACAAAT (Invitrogen). To generate an overhang for ligation-independent cloning (LIC), the PCR product was processed with DTT, dGTP (Roche), and T4 DNA polymerase (Novagen, LIC qualified) for 30 min at 22 °C and then at 75 °C for 20 min. The pMCSG7 vector,<sup>11</sup> which encodes a 6-His tag on its N-terminus, was digested with restriction enzyme SspI (New England Biolabs), processed with dCTP (Roche) and T4 DNA polymerase (Novagen, LIC qualified) for 30 min at 22 °C and then at 75 °C for 20 min. To anneal the vector with the insert, they were mixed and incubated at 22 °C for 10 min, EDTA was added, and the reaction was incubated for an additional 5 min. The mixture was used to transform *E. coli* XL-1 Blue cells (Agilent Technologies). The construct was verified by sequencing.

**Enzyme Expression.** Rosetta2 DE3 pLysS (EMD Millipore) cells were transformed with pMICAL-2 and grown with shaking at 25 °C in Luria–Bertani Broth with 100 µg/mL of ampicillin. Bacterial cultures were induced when  $A_{600} = 1$  with 1 mM IPTG and then harvested by centrifugation after 19–24 h at 15 °C. Bacterial pellets were resuspended with MICAL buffer (50 mM NaH<sub>2</sub>PO<sub>4</sub>, 100 mM NaCl, 10% glycerol, pH 7.5) and stored at –20 °C until ready to purify.

**Enzyme Purification.** After bacterial pellets were thawed, 1 mM PMSF and 5 mM 2-mercaptoethanol were added, and the mixture was sonicated for 10 min (30 s bursts followed by 1 min cooling) in an ice–salt bath.<sup>5</sup> The lysate was centrifuged for 1 h at 40 000 rpm (Beckman Ti45) at 4 °C. The supernatant was then loaded onto a nickel column (Clontec) pre-equilibrated in MICAL buffer with 5 mM 2-mercaptoethanol. To remove nonspecific binding proteins, the column was washed with MICAL buffer and 5 mM 2-mercaptoethanol, followed by MICAL buffer, 10 mM imidazole, and 5 mM 2-mercaptoethanol. To elute the enzyme, a gradient was applied starting with MICAL buffer, 10 mM imidazole, and 5 mM 2-mercaptoethanol and running to MICAL buffer, 300 mM imidazole, and 5 mM 2-mercaptoethanol. Brownish fractions were collected and pooled on the basis of their absorbance spectra, which were recorded on a Shimadzu UV-2501PC scanning spectrophotometer. Purified enzyme was concentrated (~60 µM) (Centricon, 30 kDa), exchanged into a mixture of 20 mM Na–HEPES (pH 8.0) and 1 M NaCl using Econo-Pac 10DG columns (Bio-Rad), and stored at 4 °C.

**Actin Extraction and Purification.** Actin was extracted from rabbit hind leg skeletal muscle using a published method<sup>12</sup> to make an acetone powder. To isolate actin from the acetone powder, each gram of powder was dissolved into 15 mL of buffer G (2 mM Tris–HCl, 0.1 mM CaCl<sub>2</sub>, 0.2 mM ATP, 1 mM sodium azide, 0.5 mM 2-mercaptoethanol, pH 8.0) and stirred at 4 °C for 30 min. The sample was added to a new pair of woman’s pantyhose (L’eggs Everyday knee highs, nude color) to strain the filtrate from the solid; this process was repeated twice. The filtrate was centrifuged at 10 000 rpm (Sorval SS34) for 20 min at 4 °C. The supernatant was polymerized by adding 50 mM KCl, 2 mM MgCl<sub>2</sub>, and 1 mM Na<sub>2</sub>ATP or K<sub>2</sub>ATP (Fisher, MP Biomedicals) and stirred overnight at 4 °C. The next day, more KCl was added to a final concentration of 0.8 M and stirred for 30 min at 4 °C. The sample was centrifuged for 45 min at 49 000 rpm (Beckman Ti70). Pellets were resuspended in 2 mM Tris–HCl, 0.1 mM CaCl<sub>2</sub>, 0.6 M KCl, 2 mM MgCl<sub>2</sub>, 1 mM ATP, and 0.5 mM 2-mercaptoethanol, pH 8.0, homogenized using a prechilled dounce homogenizer, and centrifuged for 60 min at 49 000 rpm

(Beckman Ti70) at 4 °C. The supernatant was dialyzed overnight in 4–6 L of 20 mM Na–HEPES, 0.2 mM ATP, 0.1 mM CaSO<sub>4</sub>, 0.5 mM 2-mercaptoethanol, pH 8.0, at 4 °C. The purity of actin was checked by SDS-PAGE (Lonza). If actin was not used immediately, it was centrifuged at 50 000 rpm (Beckman Ti70) for 90 min at 4 °C. Sucrose was added (10% w/v) to the supernatant (g-actin), and the solution was frozen, then lyophilized, and stored in a desiccator for no more than 6 months.

#### Preparation of Actin for Stopped-Flow Experiments.

Lyophilized g-actin was resuspended in water and dialyzed overnight in 6 L of 20 mM Na–HEPES, pH 8.0, at 4 °C. Actin was centrifuged at 50 000 rpm (Beckman Ti70) for 90 min at 4 °C. The concentration of g-actin in the supernatant was determined by diluting it into 8 M guanidinium and recording the absorbance spectrum (Shimadzu UV-2501PC scanning spectrophotometer). The extinction coefficient of unfolded actin (45 840 M<sup>-1</sup> cm<sup>-1</sup>) at 280 nm was calculated from the sequence using UniProtKB/Swiss-Prot database. Actin was polymerized by adding 10 mM K<sub>2</sub>SO<sub>4</sub>, 2 mM MgSO<sub>4</sub>, and 0.5 mM 2-mercaptoethanol and incubated at room temperature for ~20 min. To remove aggregates, actin was centrifuged for 10 min at room temperature at 14 500 rpm. To make polymers smaller, polymerized actin was passed through a 22-1/2 gauge needle twice.

**Synthesis of [4R-<sup>2</sup>H]NADPH.** [4R-<sup>2</sup>H]NADPH was synthesized by published methods<sup>13,14</sup> with the following modifications. Reaction mixtures had 13 mM NADP (Research Products International), 0.5 M isopropanol-*d*<sub>8</sub> (Acros Organics), and 20 units of alcohol dehydrogenase from *Thermoanaerobacter brockii* (Sigma) in a final volume of 10 mL. The buffer was 50 mM NH<sub>4</sub>HCO<sub>3</sub> adjusted to pH 7.8 with NaOH. The reaction mixture was incubated at room temperature for 2 h and monitored spectrophotometrically. Upon completion of the reaction, the mixture was added to a DEAE Sepharose Fast Flow column which had been pre-equilibrated with 50 mM NH<sub>4</sub>HCO<sub>3</sub> pH 7.8. Deuterated NADPH was removed from the column by running a gradient of 50–500 mM NH<sub>4</sub>HCO<sub>3</sub>, pH 8.5. Fractions were pooled that had a ratio of A<sub>260</sub>/A<sub>340</sub> = 2.5 or less.<sup>15</sup> The pH of the pooled fractions was adjusted to 9.8 with NH<sub>4</sub>OH. The pooled fractions were concentrated by lyophilization and stored at –20 °C.

**Reductive Half-Reaction.** The enzyme was exchanged into 20 mM HEPES with ~0.5 mM 2-mercaptoethanol, pH 8.0, using Econo-Pac 10DG columns (Bio-Rad). The reaction of the monoMICAL-2 (with or without actin) was studied in a Hi-Tech Scientific KinetAsyst SF-61 DX2 stopped-flow spectrophotometer at 4 °C. For experiments without actin, the instrument was used in its standard configuration, with a 1 cm optical path length and in dual-beam mode. For experiments that included actin, the instrument was reconfigured to a 1.5 mm optical path length and single-beam detection. Enzyme solutions were made anaerobic in a tonometer<sup>16</sup> in the presence or absence of actin and mixed with anaerobic solutions of NADPH or NADH and protio- (Research Products International) or deuterio-NADPH. The enzyme concentration after mixing ranged from 20–110 μM, actin concentrations ranged from 27–55 μM, and pyridine nucleotide concentrations were as high as 16 mM. When actin was included with the enzyme, there also was 10 mM K<sub>2</sub>SO<sub>4</sub>, 20 mM MgSO<sub>4</sub>, and 0.5 mM 2-mercaptoethanol. The oxidized flavin absorbance was recorded at 450 nm, and the charge-transfer absorbance was monitored at 550 nm. Kinetic

traces were fit to sums of exponentials using Kaleidagraph (Synergy, Inc.). The observed rate constants for flavin reduction were plotted vs NADH or NADPH concentration and fit to a square hyperbola<sup>17</sup> to obtain *k*<sub>red</sub> and *K*<sub>d</sub>.

**Reduction Potentials.** Reduction potentials were determined using enzyme (~20 μM) with or without actin (~40 μM) at 25 °C with 20 mM Na–HEPES, pH 8.0, by the method of Massey<sup>18</sup> using 1-hydroxyphenazine as an indicator dye (*E*<sub>m</sub> = –228 mV). Data were fit by a Nernst analysis of the absorbance changes of the enzyme and dye using eq 1<sup>19</sup>

$$\log \left[ \frac{A_i - A_{\text{red}}}{A_{\text{ox}} - A_i} \right]_{\text{Enz}} = (E_{m,\text{Dye}} - E_{m,\text{Enz}}) \frac{nF}{2.303RT} + \log \left[ \frac{A_i - A_{\text{red}}}{A_{\text{ox}} - A_i} \right]_{\text{Dye}} \quad (1)$$

where *n* is the number of electrons in the reduction (in this case two), *F* is Faraday's constant, *R* is the gas constant, *T* is the absolute temperature, *E*<sub>m,Dye</sub> and *E*<sub>m,Enz</sub> are the midpoint potentials of the dye and enzyme, respectively, *A*<sub>i</sub> is an absorbance during the experiment, *A*<sub>ox</sub> is an absorbance at the start of the experiment when the enzyme and dye are oxidized, and the subscripts Enz and Dye refer to absorbance values sensitive to these components, 450 and 370 nm, respectively.

**Extinction Coefficient.** Absorbance spectra were recorded of the enzyme (~20 μM) with and without 2-mercaptoethanol in 20 mM Na–HEPES, pH 8.0, before and after the addition of 0.1% SDS.<sup>20</sup> The extinction coefficient of monoMICAL-2 was determined by calculating the amount of free FAD liberated using an extinction coefficient at 449 nm of 11.3 mM<sup>-1</sup> cm<sup>-1</sup>.

## RESULTS

**General Properties.** As a starting point for studying the enzymology of the multidomain MICAL-2, we expressed and purified (as judged by SDS-PAGE) the N-terminal mono-oxygenase domain (monoMICAL-2). A reasonable amount of enzyme, 0.30 μmol, could routinely be obtained from 18 L of *E. coli* culture (170 g of cells). When the domain was purified, it was orange, not the yellow expected for most flavoenzymes. The spectrum of monoMICAL-2 (Figure 2) had absorbance at

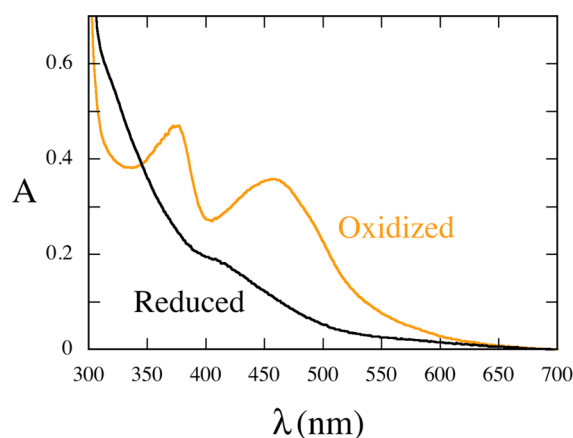


**Figure 2.** Absorbance spectrum of monoMICAL-2. The spectra of the oxidized and reduced forms of monoMICAL-2 were recorded in 20 mM HEPES, pH 8.0, at 4 °C. Note the charge-transfer absorbance above 500 nm in the oxidized enzyme.



long wavelengths where oxidized flavins normally do not absorb, which is due to a charge-transfer interaction between Trp 405 and the *re* face of the oxidized flavin.<sup>5</sup> This interaction is only possible when the flavin is in the “out” conformation. An extinction coefficient at 455 nm of  $9.8 \text{ mM}^{-1} \text{ cm}^{-1}$  was measured. We observed that high concentrations of enzyme precipitated when cold if the ionic strength of the solution was low. The precipitate could be redissolved by some combination of adding a reducing agent, NaCl, and warming.

**Reduction Potentials.** The reduction potential of monoMICAL-2 was determined by using the method of Massey.<sup>18</sup> Measurement of the reduction potentials was first attempted using the standard  $0.1 \text{ M K}_2\text{HPO}_4$ , pH 7.0 buffer; however, monoMICAL-2 precipitates in this buffer. Thus, experiments were performed in  $20 \text{ mM HEPES}$  buffer, pH 8.0. The indicator dye used was 1-hydroxyphenazine, which has a reduction potential of  $-228 \text{ mV}$  at pH 8.0.<sup>21</sup> The reduction potential of monoMICAL-2 without actin was found to be  $-240 \text{ mV}$  (Figure 3). The potential is much higher than that of

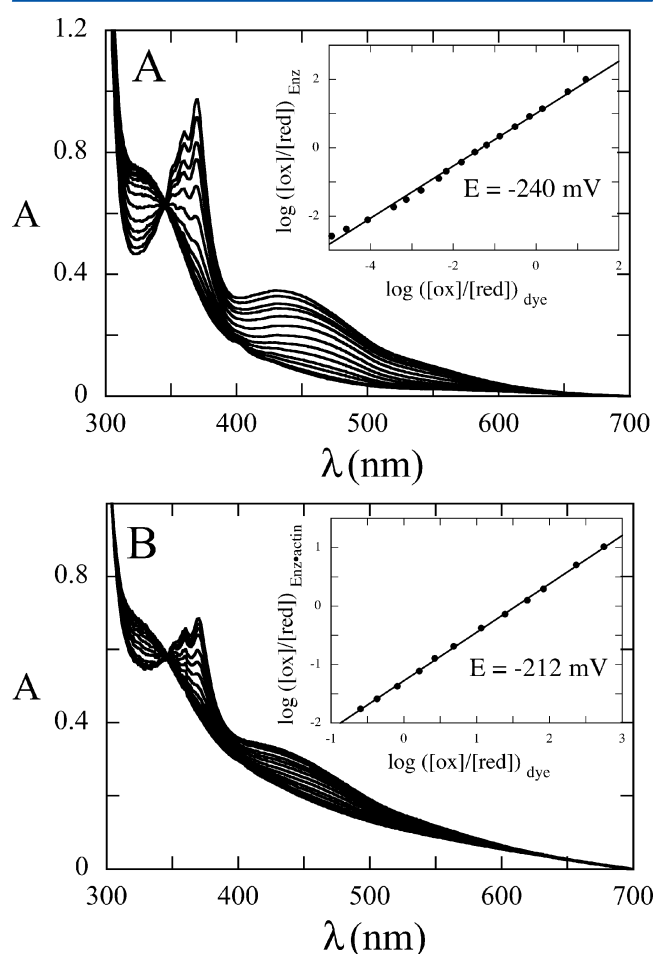


**Figure 3.** Reduction potential of monoMICAL-2. Anaerobic mixtures of enzyme and 1-hydroxyphenazine dye were slowly reduced by xanthine and xanthine oxidase in  $20 \text{ mM HEPES}$ , pH 8.0, at  $25^\circ\text{C}$ . Spectra were recorded to monitor the extent of the reduction of the dye and enzyme. These were used to determine the potential (insets). (A) monoMICAL-2 was reduced without actin, giving a potential of  $-240 \text{ mV}$ . (B) monoMICAL-2 was reduced in the presence of 1 equiv of f-actin, giving a potential of  $-212 \text{ mV}$ . Note the optical path length for the experiment in A was  $1 \text{ cm}$  and the optical path length in the experiment in B was  $0.4 \text{ cm}$ .

NADPH; therefore, the hydride-transfer reaction is essentially irreversible. The reduction potential of the monoMICAL-2·actin complex was  $-212 \text{ mV}$ . Actin raises the potential by  $\sim 30 \text{ mV}$ , giving the monoMICAL-2·actin complex a higher affinity for electrons than enzyme alone.

**Substrate-Free Reductive Half-Reaction.** Oxidized monoMICAL-2 was anaerobically mixed with varying concentrations of anaerobic NADPH in a stopped-flow instrument. Reactions were monitored by changes in absorbance of the flavin at  $450 \text{ nm}$  and fit to sums of the exponentials (Figure 4). Flavin reduction occurred in one phase. The charge-transfer

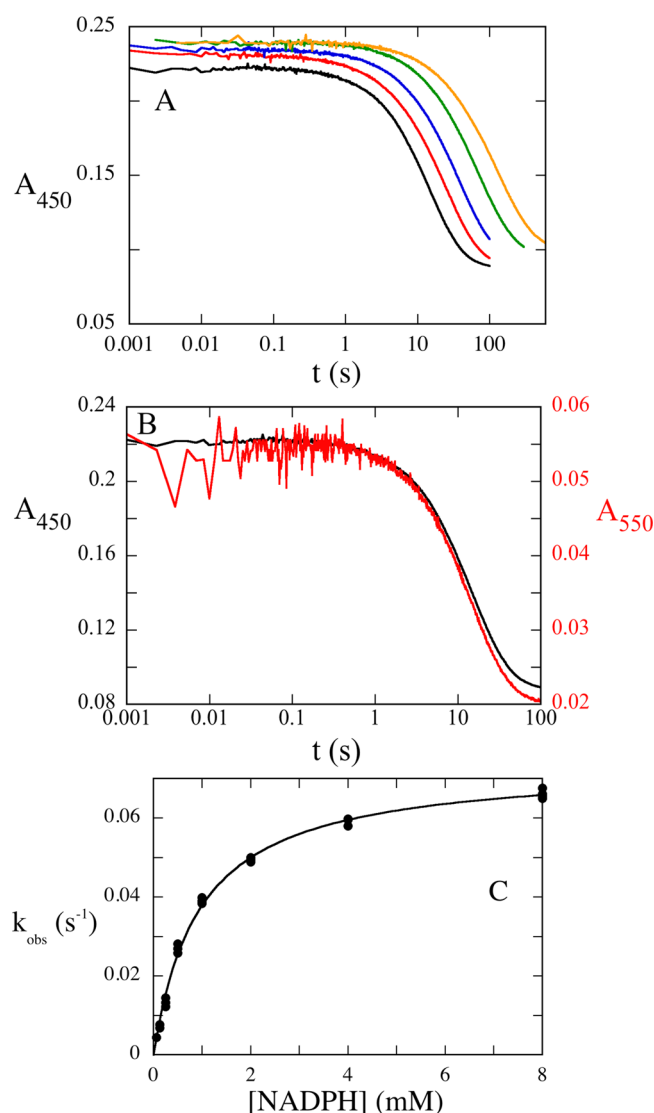
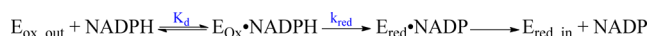


**Figure 4.** Reduction of monoMICAL-2 with NADPH. Anaerobic enzyme ( $50 \mu\text{M}$  before mixing) was mixed with anaerobic NADPH solutions in a stopped-flow spectrophotometer. All reactions were in  $20 \text{ mM HEPES}$ , pH 8.0, at  $4^\circ\text{C}$ . (A) The reduction of the enzyme was monitored at  $450 \text{ nm}$ . Note the logarithmic time scale. The concentrations of NADPH are  $8, 1, 0.5, 0.25$ , and  $0.125 \text{ mM}$ . (B) Traces for the reaction of  $8 \text{ mM NADPH}$  obtained at  $450$  and  $550 \text{ nm}$  are compared. Flavin reduction (black trace) and the disappearance of the charge-transfer complex (red trace) occur simultaneously. (C) Observed rate constants as a function of NADPH concentration were obtained by fitting the traces in A to a single exponential. These values were fit to a square hyperbola, giving  $k_{\text{red}} = 0.07 \text{ s}^{-1}$  and  $K_d = 940 \mu\text{M}$  in this experiment.

absorbance between FAD and Trp 405, observed at 550 nm, disappeared simultaneously with flavin reduction. The  $k_{\text{obs}}$  values were plotted vs concentration of NADPH, giving a square hyperbola with a  $K_d$  of  $944 \pm 39 \mu\text{M}$  and a  $k_{\text{red}}$  of  $0.074 \pm 0.0009 \text{ s}^{-1}$ . The hyperbolic dependence of  $k_{\text{obs}}$  on NADPH is most simply explained by the mechanism in Scheme 1, which

#### Scheme 1



shows reactions and flavin conformations. The experimental hyperbolic concentration dependence implies the binding of NADPH to form a complex that then reacts (first two steps in Scheme 1). The flavin of the free enzyme is assigned to the “out” conformation on the basis of the crystal structure of monoMICAL-1 and the observation of the charge-transfer absorbance in monoMICAL-2. The dissociation of NADP shown at the end of Scheme 1 was not directly observed, so it is hypothetical in this scheme, and there are no data to assign a conformation to the flavin in the NADP complex. The flavin is assigned to the “in” conformation in the final reduced enzyme on the basis of the crystal structure of monoMICAL-1. The value of  $k_{\text{red}}$  is relatively low, consistent with the behavior of an aromatic hydroxylase (Class A monooxygenase) in the absence of its substrate.

**Reduction by NADH.** To determine if MICAL-2 has a preference for NADPH or NADH, anaerobic monoMICAL-2 was mixed with different concentrations of anaerobic NADH in a stopped-flow instrument. Reduction of monoMICAL-2 was observed by monitoring the flavin absorbance at 450 nm (Figure 5). The traces were fit to a single exponential; the plot of  $k_{\text{obs}}$  vs NADH, surprisingly, looked linear. A linear increase of the observed rate constant for reduction indicates a direct bimolecular reaction of NADH with the oxidized enzyme without forming a complex. The slope of the dependence gives a bimolecular rate constant for the reaction of  $1.1 \pm 0.025 \text{ M}^{-1} \text{ s}^{-1}$ , a very low value. If, instead, a weak complex is assumed to precede the reaction, then the observed rate constant should depend hyperbolically on NADH concentration. Fitting to a square hyperbola gave a half-saturating concentration estimated to be  $53 \pm 17 \text{ mM}$ . The  $k_{\text{red}}$  was essentially the same for NADH,  $0.08 \pm 0.02 \text{ s}^{-1}$ , as for NADPH. Thus, if NADH actually does bind, MICAL-2 has a preference for NADPH over NADH due to a  $\sim 60$ -fold tighter binding. Regardless of the interpretation of these data, the 2'-phosphate of NADPH is extremely critical for binding. Interestingly, if the dependence really is hyperbolic, then the predicted  $k_{\text{red}}$  for NADH and NADPH are the same, suggesting that the same reactive complex forms.

**KIE and Stereochemistry.** Monooxygenases typically transfer the *proR* hydride of NADPH. A comparison of reduction kinetics using protio-NADPH vs  $[4\text{R-}^2\text{H}]\text{NADPH}$  was performed to determine if the same stereochemistry would be observed with monoMICAL-2. monoMICAL-2 was mixed with varying concentrations of NADPH/D (Figure 6). The  $k_{\text{red}}$  of protio-NADPH was  $0.09 \pm 0.004 \text{ s}^{-1}$ . The  $k_{\text{red}}$  for  $[4\text{R-}^2\text{H}]\text{NADPH}$  was  $0.019 \pm 0.0028 \text{ s}^{-1}$ , giving a KIE on reduction of  $4.8 \pm 0.9$ . The same KIE was obtained whether commercial or synthetic protio-NADPH was used. Thus, MICAL-2 transfers the *proR* hydride of NADPH, just like aromatic hydroxylases and other monooxygenases. The substantial KIE of 4.8 strongly suggests that hydride transfer,

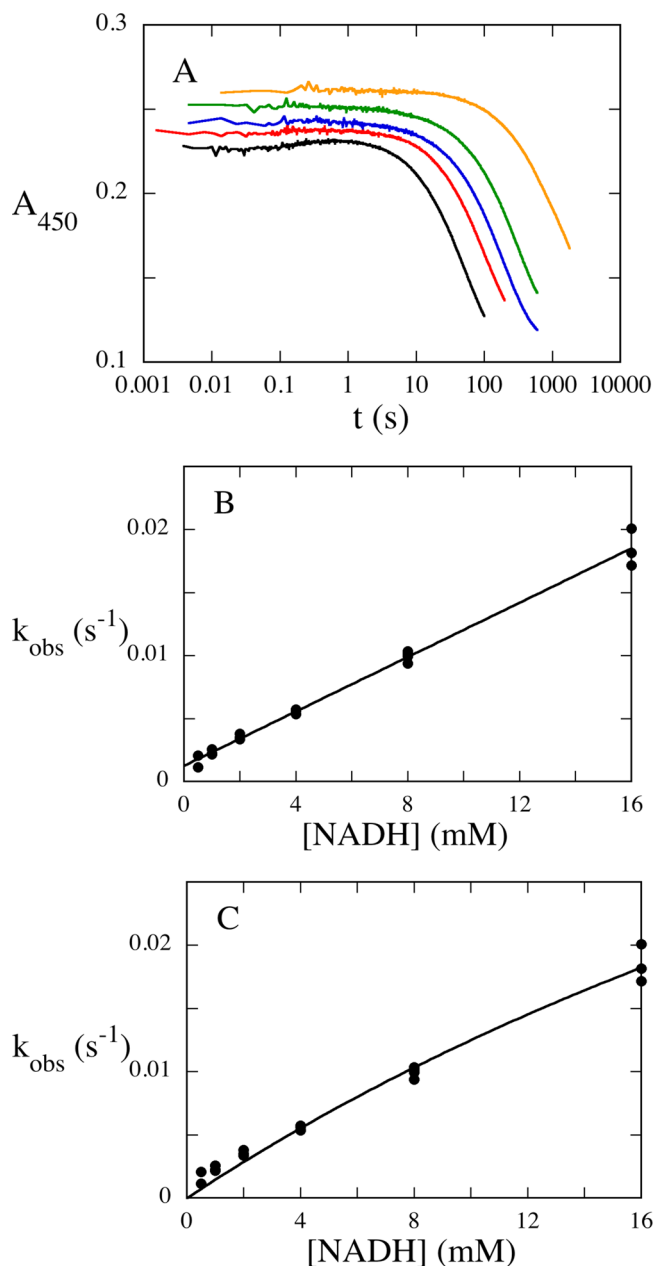


**Figure 5.** Reduction of monoMICAL-2 with NADH. Anaerobic enzyme ( $50 \mu\text{M}$  before mixing) was mixed with anaerobic NADH solutions in a stopped-flow spectrophotometer. All reactions were in  $20 \text{ mM}$  HEPES, pH 8.0, at  $4^\circ\text{C}$ . (A) The reduction of the enzyme was monitored at 450 nm. Note the logarithmic time scale. The concentrations of NADH are 16, 8, 4, 2, and  $0.5 \text{ mM}$ . (B) Observed rate constants as a function of NADH concentration were obtained by fitting the traces in A to a single exponential. These values were fit to a line, giving a bimolecular rate constant of  $1.1 \pm 0.025 \text{ M}^{-1} \text{ s}^{-1}$ . (C) The same observed rate constants were fit to a square hyperbola, giving  $k_{\text{red}} = 0.078 \text{ s}^{-1}$  and  $K_d = 53 \text{ mM}$  in this experiment. Note that the  $K_d$  and  $k_{\text{red}}$  values cannot be determined accurately.

rather than a conformational change, controls the rate constant of reduction when actin is not bound. Therefore, the charge-transfer absorbance disappears because of chemistry, rather than movement of the flavin away from Trp 405.

**Reduction in the Presence of Actin.** The substrate for monoMICAL is f-actin.<sup>5,10,22</sup> Experiments were performed to study the reduction of monoMICAL-2 in the presence of f-

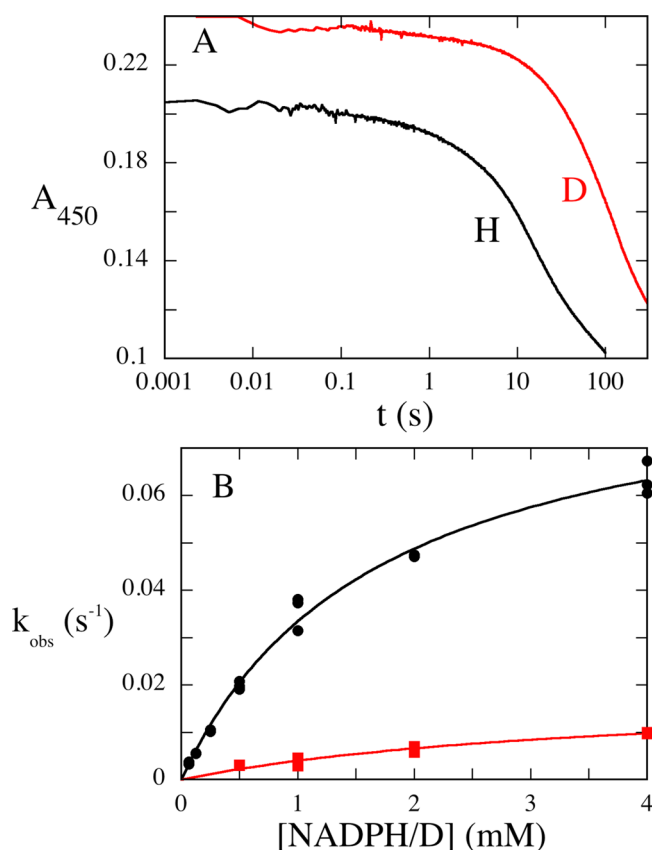


**Figure 6.** KIE on the reduction of monoMICAL-2. Reactions using either protio-NADPH or  $[4R\text{-}^2H]\text{NADPH}$  were performed as described in Figure 3. (A) Stopped-flow traces at 450 nm are shown comparing the reduction by 4 mM (after mixing) deuterio-NADPH in red and 4 mM (after mixing) protio-NADPH in black. (B) The observed rate constants varied with NADPH/D concentration. The values for  $k_{\text{red}}$  were obtained by fitting to a square hyperbola, giving a KIE of  $4.8 \pm 0.9$ .

actin. Our initial attempts at stopped-flow experiments were not successful; the binding of actin to monoMICAL-2 appears to be weak, but increasing the concentration of actin obliterated the absorbance signal due to turbidity. Also, our preparations of actin had a significant amount of actin aggregates, which caused erratic signal changes. To address these challenges, the stopped-flow instrument was reconfigured to use a 1.5 mm path length to allow us to increase our concentration of actin but still be within the detection limit of the instrument. This improved the quality of the data but did not eliminate the variable background of light scattering. In our most successful experiments, freshly polymerized actin (110–220  $\mu\text{M}$ ) was passed twice through a 22-1/2 gauge needle to help break up aggregates. This was then incubated with monoMICAL-2 (40–220  $\mu\text{M}$ ) anaerobically and mixed 1:1 with different concentrations of NADPH in the same buffer. Reduction was monitored by observing the change in the flavin absorbance at 450 and 550 nm (Figure 7). Three phases were observed, with the first phase being most prone to interference by scattering. To confirm the presence of three reaction phases, traces from 450 and 550 nm were used to plot trajectories in a phase plane (Figure 7B). Phase planes are classically used in the analysis of dynamical trajectories whose coordinates are dependent variables in ordinary time-dependent differential equations. Phase planes apparently have not been employed yet to analyze

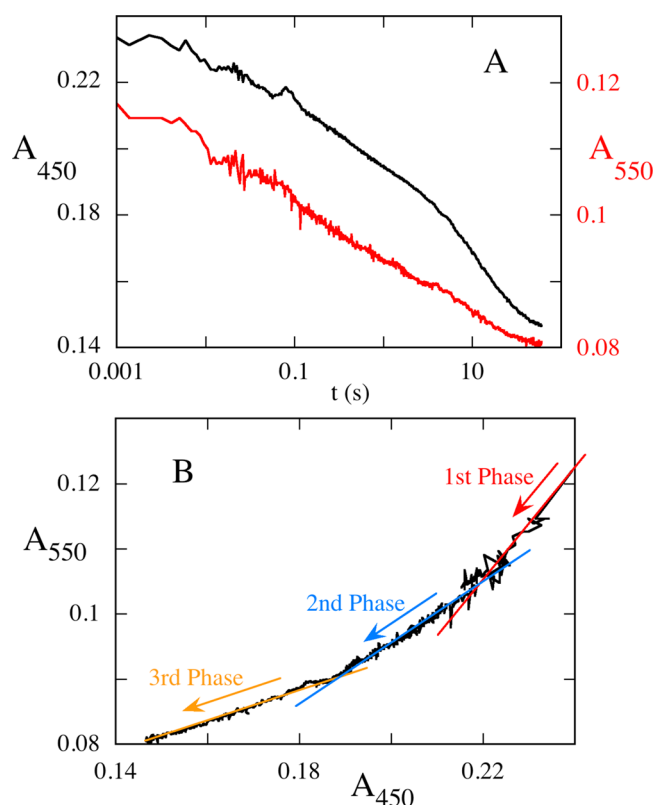
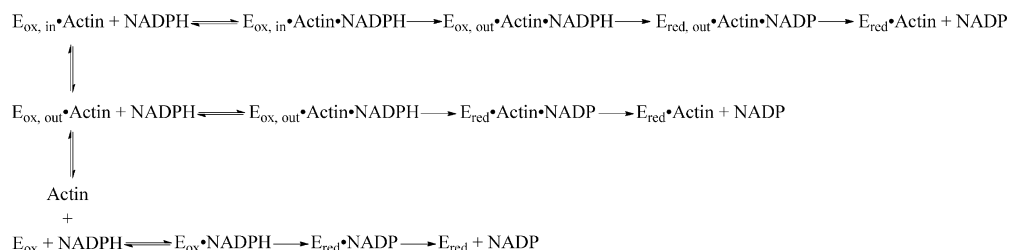


**Figure 7.** Kinetics of reduction of monoMICAL-2 in the presence of f-actin. (A) Stopped-flow traces are shown for the reaction of a mixture of oxidized monoMICAL-2 and f-actin with NADPH (4 mM after mixing) in the absence of  $\text{O}_2$  in 20 mM Na-HEPES, pH 8.0, 4  $^\circ\text{C}$ . Traces collected at 450 nm (black) and 550 nm (red) are shown. Note the logarithmic time scale. (B) The absorbance trajectory defined by the traces in A is plotted on a phase plane. The trajectory starts in the upper right part of the plot and moves downward and to the left. Linear segments identifying the three reaction phases are indicated in red, blue, and orange for the first, second, and third phases, respectively.

stopped-flow data but offer a simple way to determine whether spectral changes observed at different wavelengths are caused by the same reactions, different reactions, or random scattering events. As applied here (Figure 7B), the coordinates of the trajectory are  $(A_{450}, A_{550})$ , and each coordinate is dependent on the parametric variable time; this is analogous to the time dependence of spatial coordinates of a moving particle in classical mechanics. Although each  $(A_{450}, A_{550})$  point corresponds to a certain reaction time, time is not plotted on the phase plane. In pseudo-first-order reactions, the time dependence of the system is controlled by exponentials. If the absorbance change at each wavelength is caused by the same reaction, the trajectory in the phase plane will be linear because the same exponential controls the evolution of both absorbances. Multiple phases will appear as connected line segments. However, if absorbance changes are controlled by different observed rate constants, curved trajectories will be obtained, and changes caused by randomly fluctuating aggregates should give random trajectories. The trajectory of  $(A_{450}, A_{550})$  plotted in Figure 7B for the reaction of 4 mM NADPH is composed of three connected line segments, indicating three reaction phases, confirming the conclusions from the analysis of the individual traces. The first reaction phase, 11% of total reduction, was most subject to interference

Scheme 2



by light scattering, but we could still estimate that the rate constant for reduction is  $120 \pm 30 \text{ s}^{-1}$ . The second phase, 46% of total reduction, had a limiting rate constant of  $2.1 \pm 0.2 \text{ s}^{-1}$ . The third phase, 43% of total reduction, had essentially the same kinetics observed in experiments without actin ( $k_{red}$  of  $0.088 \pm 0.004 \text{ s}^{-1}$ ) and a  $K_d$  consistent with that measured in the reaction without actin. This phase is ascribed to the reaction of actin-free monoMICAL-2. The reactions occurring in these experiments are explained by Scheme 2, which shows the independent reduction of three enzyme populations: two with actin bound and one without.

## DISCUSSION

MICAL, a large protein of  $\sim 1000$  residues, causes actin to depolymerize. Its N-terminus is a flavin monooxygenase domain and is followed by several protein–protein interaction domains. The monooxygenase domain is vital for motor axons to be properly guided during embryonic development.<sup>3,23</sup> In order to understand how MICALs perform their biological roles, detailed enzymological studies are needed on the mechanism of the monooxygenase half-reactions.

There are many classes of monooxygenases, Class A–F;<sup>7</sup> monoMICAL-2 has been classified, on the basis of its sequence and the structure of monoMICAL-1, as an aromatic monooxygenase, Class A. monoMICAL-1 has one Rossmann fold, for binding FAD, the same as Class A. In contrast, the structure and sequences of monoMICALs are very different from those of the Class B monooxygenases. Class B has two Rossmann folds, one for binding FAD and another for binding pyridine nucleotides. The flavins of aromatic hydroxylases (Class A) change conformation from “in” to “out”, whereas those in Class B do not. The oxidized flavin of monoMICAL-1 adopts an “out” conformation,<sup>8,9</sup> where it is more exposed to solvent, and when it is reduced, it moves to the “in” conformation, where it is partly buried in the protein. The high sequence identity between monoMICAL-2 and monoMICAL-1 (60% using Lalign<sup>24</sup>) strongly suggests that the structure of monoMICAL-2 will be very similar to that of monoMICAL-1, allowing the structure of monoMICAL-1 to guide our interpretations. This idea is strongly supported by the FAD–Trp charge-transfer absorbance of monoMICAL-2, which was first reported for human monoMICAL-1<sup>5</sup> and *Drosophila* MICAL.<sup>3</sup> Also, mutating Trp 405 to Ala in monoMICAL-2 eliminates the charge-transfer absorbance (unpublished). Thus, from a structural perspective, monoMICAL-2 seems to be an aromatic hydroxylase. However, MICAL oxygenates the sulfur of a methionine side chain.<sup>10</sup> The oxidation of thioethers is a classic reaction performed by Class B enzymes but not by aromatic hydroxylases.<sup>6</sup> We performed experiments to determine how similar enzymatically monoMICAL-2 is to the aromatic hydroxylases.

There are two key differences between the reductive half-reactions of Class A and Class B enzymes:<sup>6</sup> Class A enzymes are stimulated by their substrate, whereas Class B enzymes are always stimulated, even in the absence of substrate; the flavin in Class A enzymes moves to the “out” conformation in order to react with NAD(P)H, whereas the flavin of Class B enzymes is stationary. When f-actin (the reported substrate of MICAL<sup>10</sup>) was added to the reductive half-reaction in our experiments, monoMICAL-2 was stimulated by as much as  $\sim 10^3$ -fold. The presence of actin created two new phases that were faster than the reaction of free monoMICAL-2, showing that two different enzyme-actin complexes were present. The fastest phase was not defined accurately due to the optical interference caused by actin, but it is faster than free enzyme by about 3 orders of magnitude. The second phase is faster than free enzyme by about 1 order of magnitude. The two faster populations of enzyme might be attributed to actin bound to enzyme with the flavin in both the “in” and “out” conformations. The flavins of aromatic hydroxylases (Class A) react when in the “out” conformation. Therefore, we propose that the fastest phase is caused by reduction of oxidized enzyme in the “out” conformation with actin bound, and the second phase is due to the slower reaction of oxidized monoMICAL-2 in the “in” conformation with actin bound. A possible explanation for the two actin complexes is that the missing C-terminal protein–protein interacting domains might be needed to favor the actin complex with the flavin in the more reactive “out” conformation.

The flavins of Class A enzymes react with NAD(P)H in the “out” conformation, and then their flavins move to the “in” conformation. The substantial KIE and synchronization of reduction with the disappearance of the charge transfer shows that reduction happens in the “out” conformation, as with other aromatic hydroxylases. Subsequently, the reduced flavin moves to the “in” conformation seen in the crystal structure. Interestingly, reduction is slow for monoMICAL-2 even when the flavin is in the “out” conformation, which would allow full access by NADPH; something other than access is responsible for slow reduction and is relieved by f-actin. Some PHBH mutants act this way too.<sup>25</sup>

Our results contradict several published ideas about how MICAL controls its reactivity with NADPH. Nadella et al. reported<sup>9</sup> a high oxidase activity for monoMICAL-1 ( $77 \text{ s}^{-1}$ ) without control by substrate or protein–protein interaction domains, obtained by the Amplex Red assay for  $\text{H}_2\text{O}_2$ . This would require a  $k_{red}$  greater than  $77 \text{ s}^{-1}$ , not slow as we report here or as was reported for monoMICAL-1.<sup>5</sup> Zucchini et al. showed that the Amplex Red reaction is artifactually fast.<sup>5</sup> We have found resorufin, the product of the Amplex Red reaction, reacts with the enzyme in a complex radical chain (unpublished). Schmidt et al. proposed that the C-terminal domains of MICAL-1 inhibit the reactivity of the monoox-



xygenase domain,<sup>26</sup> but the experimental data supporting these ideas seem inadequate to determine how this could happen. The steady-state assays of the oxidase activity used in that study were only semiquantitative, not allowing a  $k_{\text{cat}}$  (and, therefore, a lower limit on  $k_{\text{red}}$ ) to be determined. Much of the work was done with crude preparations rather than with purified proteins, and some of the experiments used the artifactual Amplex Red assay or included high concentrations of  $\text{Cl}^-$ , an inhibitor of aromatic hydroxylases. Therefore, although it is possible that C-terminal domains, or another protein such as collapsin response mediator proteins, could inhibit the reduction of monoMICAL, definitive enzymology has yet to be done.

## CONCLUSION

Our data show that monoMICAL-2 has the classic regulatory behavior of flavin-dependent aromatic hydroxylases even without the protein–protein interaction domains. However, it is not like aromatic hydroxylases in its substrate preference,<sup>10</sup> where it behaves like a Class B enzyme that oxygenates nonaromatics. monoMICAL-2 has behaviors of both families of enzymes. This would be the first time a Class A flavin monooxygenase oxygenates a thioether. monoMICAL-2 is partly an aromatic hydroxylase and partly a Class B enzyme.

## AUTHOR INFORMATION

### Corresponding Author

\*B.A.P. E-mail: brupalf@umich.edu. Phone: (734) 615-2452. Fax: (734) 764-3509.

### Funding

†C.A.M. was supported by University of Michigan Rackham Merit Fellowship and a Rackham Predoctoral Fellowship.

### Notes

The authors declare no competing financial interest.

## ACKNOWLEDGMENTS

We thank Matthew Deitz and Jacob Talhelm for help in preparations of actin and Nancy Roeser for the bunny bodies. We also thank Professors Ann Miller (University of Michigan), Ken Johnson (University of Texas, Austin), Steve Almo (Albert Einstein Medical School), and Kevin Sonnemann, Ph.D. (University of Wisconsin—Madison), for their advice on preparing actin for stopped-flow experiments. We thank Professor Pablo Sobrado (Virginia Tech) for providing samples of protio- and deuterio-NADPH and Professor Patrick O'Brien (University of Michigan) for helpful comments on the manuscript. We also thank Professor Maria A. Vanoni (Università degli Studi di Milano) for helpful advice on enzyme purification.

## ABBREVIATIONS

MICAL, molecule interacting with CasL; monoMICAL, monooxygenase domain of MICAL; KIE, kinetic isotope effect; CH, calponin homology domain; LIM, gene products Lin1-1, Isl-1, and Mec-3; PHBH, *p*-hydroxybenzoate hydroxylase; LIC, ligation-independent cloning; DTT, dithiothreitol; SDS, sodium dodecyl sulfate; PAGE, polyacrylamide gel electrophoresis

## REFERENCES

(1) Pak, C. W., Flynn, K. C., and Bamberg, J. R. (2008) Actin-binding proteins take the reins in growth cones. *Nat. Rev. Neurosci.* 9, 136–147.

(2) Zhou, Y., Gunput, R. A., Adolfs, Y., and Pasterkamp, R. J. (2011) MICALs in control of the cytoskeleton, exocytosis, and cell death. *Cell. Mol. Life Sci.* 68, 4033–4044.

(3) Terman, J. R., Mao, T., Pasterkamp, R. J., Yu, H. H., and Kolodkin, A. L. (2002) MICALs, a family of conserved flavoprotein oxidoreductases, function in plexin-mediated axonal repulsion. *Cell* 109, 887–900.

(4) Ashida, S., Furihata, M., Katagiri, T., Tamura, K., Anazawa, Y., Yoshioka, H., Miki, T., Fujioka, T., Shuin, T., Nakamura, Y., and Nakagawa, H. (2006) Expression of novel molecules, MICAL2-PV (MICAL2 prostate cancer variants), increases with high Gleason score and prostate cancer progression. *Clin. Cancer Res.* 12, 2767–2773.

(5) Zucchini, D., Caprini, G., Pasterkamp, R. J., Tedeschi, G., and Vanoni, M. A. (2011) Kinetic and spectroscopic characterization of the putative monooxygenase domain of human MICAL-1. *Arch. Biochem. Biophys.* 515, 1–13.

(6) Palfey, B. A., and McDonald, C. A. (2010) Control of catalysis in flavin-dependent monooxygenases. *Arch. Biochem. Biophys.* 493, 26–36.

(7) van Berkel, W. J., Kamerbeek, N. M., and Fraaije, M. W. (2006) Flavoprotein monooxygenases, a diverse class of oxidative biocatalysts. *J. Biotechnol.* 124, 670–689.

(8) Siebold, C., Berrow, N., Walter, T. S., Harlos, K., Owens, R. J., Stuart, D. I., Terman, J. R., Kolodkin, A. L., Pasterkamp, R. J., and Jones, E. Y. (2005) High-resolution structure of the catalytic region of MICAL (molecule interacting with CasL), a multidomain flavoenzyme-signaling molecule. *Proc. Natl. Acad. Sci. U. S. A.* 102, 16836–16841.

(9) Nadella, M., Bianchet, M. A., Gabelli, S. B., Barrila, J., and Amzel, L. M. (2005) Structure and activity of the axon guidance protein MICAL. *Proc. Natl. Acad. Sci. U. S. A.* 102, 16830–16835.

(10) Hung, R. J., Pak, C. W., and Terman, J. R. (2011) Direct redox regulation of F-actin assembly and disassembly by Mical. *Science* 334, 1710–1713.

(11) Stols, L., Gu, M., Dieckman, L., Raffin, R., Collart, F. R., and Donnelly, M. I. (2002) A new vector for high-throughput, ligation-independent cloning encoding a tobacco etch virus protease cleavage site. *Protein Expression Purif.* 25, 8–15.

(12) Pardee, J. D., and Spudich, J. A. (1982) Purification of muscle actin. *Methods Enzymol.* 85 (Pt B), 164–181.

(13) Ottolina, G., Riva, S., Carrea, G., Danieli, B., and Buckmann, A. F. (1989) Enzymatic synthesis of [4R-2H]NAD (P)H and [4S-2H]NAD(P)H and determination of the stereospecificity of 7  $\alpha$ - and 12  $\alpha$  hydroxysteroid dehydrogenase. *Biochim. Biophys. Acta* 998, 173–178.

(14) Rider, L. W., Ottosen, M. B., Gattis, S. G., and Palfey, B. A. (2009) Mechanism of dihydrouridine synthase 2 from yeast and the importance of modifications for efficient tRNA reduction. *J. Biol. Chem.* 284, 10324–10333.

(15) Wu, J. T., Wu, L. H., and Knight, J. A. (1986) Stability of NADPH: effect of various factors on the kinetics of degradation. *Clin. Chem.* 32, 314–319.

(16) Palfey, B. A. (2003) in *Time Resolved Spectral Analysis* (Johnson, K. A., Ed.), pp 203–207, Oxford University Press, New York.

(17) Strickland, S., Palmer, G., and Massey, V. (1975) Determination of dissociation constants and specific rate constants of enzyme-substrate (or protein-ligand) interactions from rapid reaction kinetic data. *J. Biol. Chem.* 250, 4048–4052.

(18) Massey, V. (1990) in *Flavins and Flavoproteins* (Curti, B., Ronchi, S., and Zanetti, G., Ed.), pp 59–66, Walter de Gruyter, Berlin, Germany.

(19) Minnaert, K. (1965) Measurement of the equilibrium constant of the reaction between cytochrome c and cytochrome a. *Biochim. Biophys. Acta* 110, 42–56.

(20) Entsch, B., Palfey, B. A., Ballou, D. P., and Massey, V. (1991) Catalytic function of tyrosine residues in para-hydroxybenzoate hydroxylase as determined by the study of site-directed mutants. *J. Biol. Chem.* 266, 17341–17349.



- (21) Clark, W. M. (1960) *Oxidation-Reduction Potentials of Organic Systems*, The Williams & Wilkins Company, Baltimore, MD.
- (22) Hung, R. J., Yazdani, U., Yoon, J., Wu, H., Yang, T., Gupta, N., Huang, Z., van Berkel, W. J., and Terman, J. R. (2010) Mical links semaphorins to F-actin disassembly. *Nature* 463, 823–827.
- (23) Landgraf, M., Bossing, T., Technau, G. M., and Bate, M. (1997) The origin, location, and projections of the embryonic abdominal motoneurons of *Drosophila*. *J. Neurosci.* 17, 9642–9655.
- (24) Huang, X. Q., and Miller, W. (1991) A Time-Efficient, Linear-Space Local Similarity Algorithm. *Adv. Appl. Math.* 12, 337–357.
- (25) Moran, G. R., Entsch, B., Palfey, B. A., and Ballou, D. P. (1996) Evidence for flavin movement in the function of p-hydroxybenzoate hydroxylase from studies of the mutant Arg220Lys. *Biochemistry* 35, 9278–9285.
- (26) Schmidt, E. F., Shim, S. O., and Strittmatter, S. M. (2008) Release of MICAL autoinhibition by semaphorin-plexin signaling promotes interaction with collapsin response mediator protein. *J. Neurosci.* 28, 2287–2297.